

# Magnetic hysteresis properties of interacting and noninteracting micron-sized magnetite produced by electron beam lithography

**Adrian R. Muxworthy**

*GeoForschungsZentrum Potsdam, Telegrafenberg, D-14473 Potsdam, Germany*

*Permanently at Department of Earth Science and Engineering, Imperial College, South Kensington Campus, London SW7 2AZ, UK (adrian.muxworthy@imperial.ac.uk)*

**James G. King**

*Department of Physics, University of Botswana, Gaborone, Private Bag UB 00704, Botswana*

**Nic Odling**

*Grant Institute of Earth Sciences, University of Edinburgh, Kings Buildings, West Mains Road, Edinburgh EH9 3JW, UK*

[1] The magnetic hysteresis properties for well-defined micron-sized magnetite samples produced by electron beam lithography (EBL) are presented. In addition to measuring standard hysteresis parameters, first-order reversal curve (FORC) diagrams are also reported. EBL produces samples that consist of particles with very tightly constrained size distributions, and spatial distributions that govern the degree of intergrain magnetostatic interactions are accurately controlled and known. Thus EBL samples are significantly better characterized compared to powdered samples, which are conventionally used to characterize the size dependency of magnetic hysteresis properties of naturally occurring magnetic minerals. Compared with the hysteresis properties of powdered samples of the same nominal sizes, EBL samples display more multidomain-like (MD) behavior. The influence of magnetostatic interactions fields on hysteresis properties is analyzed. When magnetostatic interactions are effectively in only one direction, the hysteresis properties become more single domain-like, and if the interactions are in more than one direction, hysteresis becomes more MD-like, in agreement with numerical models.

**Components:** 3835 words, 5 figures, 1 table.

**Keywords:** electron beam lithography; magnetite; hysteresis; pseudo-single domain; FORC.

**Index Terms:** 1540 Geomagnetism and Paleomagnetism: Rock and mineral magnetism; 1512 Geomagnetism and Paleomagnetism: Environmental magnetism; 1517 Geomagnetism and Paleomagnetism: Magnetic anomalies: modeling and interpretation.

**Received** 17 March 2006; **Revised** 11 May 2006; **Accepted** 30 May 2006; **Published** 25 July 2006.

Muxworthy, A. R., J. G. King, and N. Odling (2006), Magnetic hysteresis properties of interacting and noninteracting micron-sized magnetite produced by electron beam lithography, *Geochem. Geophys. Geosyst.*, 7, Q07009, doi:10.1029/2006GC001309.

## 1. Introduction

[2] There is a growing requirement in paleo- and environmental magnetism to understand the relationship between the magnetic signal of a mineral and its grain-size properties. For example, paleoclimatic information is often revealed by subtle changes in grain-size distribution, while the same grain-size variations can complicate determination of the relative paleofield intensity from the same sediments.

[3] The relationship between grain size and magnetic signature is highly complex, particularly near size-dependent transitions between different types of magnetic domain state, e.g., single domain (SD) to multidomain (MD), where there is an abrupt change in the magnetic properties. Characterizing the magnetic behavior near these critical sizes has historically been achieved both numerically and experimentally, however, both approaches have their limitations. Numerical models can often be over simplified and limited by available computing capacity. Experimental studies are strongly dependent on the quality and character of the samples. Features which can strongly affect sample behavior are (1) stoichiometry, (2) shape and width of grain-size distributions, and (3) spatial distributions of the magnetic particles. Closely spaced grains can give rise to intergrain magnetostatic interactions, which are known to strongly affect behavior [e.g., Dunlop *et al.*, 1990; Muxworthy *et al.*, 2003].

[4] Most previous experimental rock-magnetic studies have used powdered samples to investigate grain-size dependencies [e.g., Day *et al.*, 1977; Yu *et al.*, 2004]. Powdered samples commonly have wide grain-size distributions, and are difficult to disperse giving rise to high-levels of magnetostatic interactions even when distributed in a nonmagnetic matrix. This dispersion problem is particularly common for small SD or pseudo-single domain (PSD) grains, which have a tendency to “clump.” The wide grain-size distributions and magnetostatic interactions associated with powder samples make it difficult to quantify the “true” grain-size dependency for noninteracting grains.

[5] In the last 10–15 years it has been possible to produce samples with two dimensional arrays of identically sized particles and controlled spatial distributions using various electron beam lithographic (EBL) techniques [e.g., King *et al.*, 1996; Fernandez *et al.*, 1998]. EBL uses an electron beam writer to create patterns on thin films, and produces samples with very tight grain-size distri-

bution and controlled/known spatial distributions. Although many EBL studies have been made, only one study has produced magnetite [King, 1996; King *et al.*, 1996; King and Williams, 2000], arguably the most important geological magnetic mineral.

[6] In this paper we report the magnetic hysteresis behavior of six micron magnetite particle arrays produced using EBL by King [1996]. In addition to standard magnetic hysteresis parameters coercive force  $H_C$ , remanent coercive force  $H_{CR}$ , saturation magnetization  $M_S$  and the saturation remanence  $M_{RS}$  needed to produce “Day plots” [Day *et al.*, 1977], we report first-order-reversal-curve (FORC) diagrams for these well-defined samples.

[7] By measuring samples produced by EBL we remove the problem of grain-size distribution and unquantified magnetostatic-interaction effects associated with powdered samples. Such constrained samples are ideal for testing theoretical and numerical models, though the EBL samples can sometimes suffer from crystallographic interactions between the magnetic material and the substrate [Pan *et al.*, 2002], and the magnetic grains themselves can be polycrystalline. Annealing reduces the degree of polycrystallinity. The samples discussed in this paper were initially annealed on production, and then reannealed as part of this study.

## 2. Sample Description

[8] The six EBL samples were manufactured by King [1996]. Although stored in alcohol, it is possible that the samples had been partially oxidized by atmospheric oxygen. To ensure magnetite stoichiometry, the samples were annealed in a  $\text{CO}_2$ -5% $\text{H}_2$  atmosphere at 600°C for 8 hours. The state of the samples was then checked using scanning electron microscopy (SEM). SEM observations found ~5–10% of grains had lifted off from the substrate during the reduction process, leaving a few random gaps in the arrays and breaking the symmetries of the grain distributions. The remaining grains were in good condition after reduction.

[9] Their physical properties are summarized in Table 1. All the samples were greater than one micron in size, i.e., an order of magnitude above the critical SD to MD transition size. Such grain sizes are typically thought to display pseudo-single domain (PSD) behavior [e.g., Day *et al.*, 1977; Yu *et al.*, 2004].

Table 1. Physical and Magnetic Hysteresis Properties of the Six Samples<sup>a</sup>

Sample Name	Grain Size, <sup>b</sup> $\mu\text{m}$	Spacing, $\mu\text{m}$	Parallel			45°			Perpendicular		
			$\mu_0 H_C$ , mT	$\mu_0 H_{CR}$ , mT	$M_{RS}/M_S$	$\mu_0 H_C$ , mT	$\mu_0 H_{CR}$ , mT	$M_{RS}/M_S$	$\mu_0 H_C$ , mT	$\mu_0 H_{CR}$ , mT	$M_{RS}/M_S$
<i>S1</i>	$1 \times 1 \times 1$	$3.5 \times 3.5$	8.2	23	0.14	...	...	8.3	24	0.15	
<i>S2</i>	$1 \times 1 \times 1$	$2.5 \times 2.5$	8.4	29	0.12	...	...	8.3	27	0.12	
<i>S3</i>	$1 \times 1 \times 1$	$1.5 \times 1.5$	3.9	12	0.09	...	...	4.1	13	0.08	
<i>A1</i>	$3 \times 1 \times 1$	$10 \times 11$	6.9	18	0.17	...	...	5.8	15	0.12	
<i>A2</i>	$3 \times 1 \times 1$	$1 \times 2.5$	12	39	0.20	...	...	7.4	28	0.13	
<i>A3</i>	$4 \times 3 \times 1$	$7 \times 6$	3.9	14	0.07	...	...	3.6	16	0.06	

<sup>a</sup>The grain sizes were confirmed by scanning electron micrographs. Parallel, 45°, and perpendicular magnetic measurements refer to the direction of the applied field with respect to the long axis of the grains with the sample. The depth for all the grains was 1  $\mu\text{m}$ ; e.g., *A2* has dimensions of  $3 \times 1 \times 1 \mu\text{m}$ , and *A3* has dimensions of  $4 \times 3 \times 1 \mu\text{m}$ .  
<sup>b</sup>Last number refers to the depth of the sample out of the thin-film plane.

[10] Samples *S1*, *S2* and *S3* were symmetrical both in grain shape and spatial distribution. The grains on each sample were regular 1  $\mu\text{m}$  cubes, and each sample had a different intergrain spacing (Table 1). Images of these samples are depicted by King [1996] and King *et al.* [1996]. Numerical hysteresis simulations for PSD grains suggest that sample *S1* should have been effectively noninteracting, and *S3* subject to moderate interaction fields [Muxworthy *et al.*, 2003]. Samples *A1*, *A2* and *A3* were asymmetrical both in terms of grain shape and spatial distribution. Samples *A1* and *A2* have identically shaped grains, i.e.,  $3 \times 1 \times 1 \mu\text{m}$ . The grains in *A1* were effectively noninteracting, while in *A2* strongly interacting, but only in one direction; the direction of the grain elongation. Plate-like sample *A3* was a little larger in size than the other five samples ( $4 \times 3 \times 1 \mu\text{m}$ ), and although asymmetrical in terms of both grain shape and spacing, the asymmetry in the plane of measurement, i.e.,  $4 \times 3 \mu\text{m}$ , was quite small. This larger sample was thought to be effectively noninteracting.

[11] From the spatial distributions, samples *S3* and *A2* were the most likely to be influenced by magnetostatic interactions, however, there is fundamental difference in the effect of the interactions fields in the two systems. In sample *S3*, the interaction fields were symmetrical in the plane of measurement, i.e., a two-dimensional (planar) interaction field, whereas in *A2* the interaction field was predominantly in the direction of the particle elongation, i.e., linear interaction field. Planar interaction fields have been shown numerically to make SD assemblages more MD-like, while linear interactions fields more SD-like [Muxworthy and Williams, 2004].

### 3. Hysteresis Behavior and the Day Plot

[12] The magnetic hysteresis behavior of the samples was measured using a Princeton Measurements alternating gradient magnetometer. This instrument is of sufficient sensitivity to measure the magnetic characteristics of the small number of magnetic particles (50,000 to 100,000) on each sample. All the hysteresis measurements were made in the plane of the thin films. Samples with asymmetrical particles and spatial distributions were measured in three directions, i.e., both parallel and perpendicular to the long grain axis and at  $\sim 45^\circ$ . This procedure was repeated for the symmetrical samples, but no significant difference was found between the parallel and perpendicular

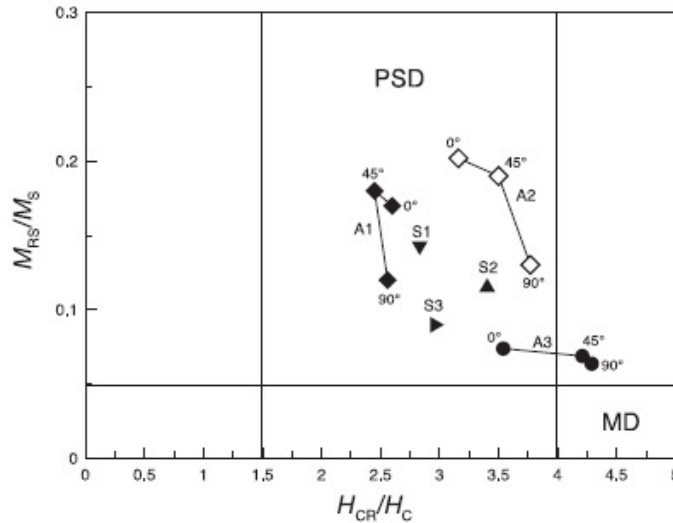


Figure 1. A Day plot of  $M_{RS}/M_S$  versus  $H_{CR}/H_C$  for the six samples in this study. The asymmetric samples *A1*, *A2*, and *A3* have been measured parallel ( $0^\circ$ ), at  $45^\circ$ , and perpendicular ( $90^\circ$ ) to their elongated grain axis (Table 1). The symmetric samples were measured both parallel and perpendicular to the field (Table 1). Only their parallel data are shown in this figure.

measurements. Standard hysteresis parameters are displayed in Table 1.

### 3.1. “Noninteracting” Samples

[13] It is difficult to compare directly the three (weakly or) noninteracting samples, i.e., *S1*, *A1* and *A3*, due to their different grain shapes, i.e., respectively cube, rod and plate, however, the coercivity and the  $M_{RS}/M_S$  ratio are seen to decrease with increasing grain volume (Table 1).

[14] Both the asymmetric samples display hysteresis parameters that are dependent on orientation. Both display increased coercive force and  $M_{RS}/M_S$  values for the field applied along the long axis, compared to measurements perpendicular to the long axis, e.g., for *A1* the coercive force increases from 5.8 mT to 6.9 mT. The effect is far more pronounced in *A1* compared to *A3*, which reflects both the size difference between the samples and the relative elongation. *A3* has only an elongation ratio  $q$  (long-axis/short-axis) of 1.3, compared to  $q = 3.0$  in sample *A1*. Both grains are above the SD/MD threshold. The effects of shape are more important in SD systems.

[15] When the hysteresis parameters are plotted on the Day plot, i.e.,  $M_{RS}/M_S$  versus  $H_{CR}/H_C$ , the

three noninteracting samples plot near the PSD/MD boundary (Figure 1). In samples *A1* and *A3* measurement of the hysteresis perpendicular to the direction of elongation produces a more MD-like signal compared to the measurements parallel to the elongation. The hysteresis data measured at  $45^\circ$  are approximately intermediate to the measurements at  $0^\circ$  and  $90^\circ$ , though the intermediate measurement for *A1* is more SD-like.

### 3.2. Influence of Magnetostatic Interactions

[16] The role of interactions is clearly demonstrated in the samples. In the sample sequence *S1*, *S2* and *S3*, the spacing between identical  $1 \mu\text{m}$  cubic grains decreases. There is a change in the hysteresis parameters between *S2* and *S3*, with a significant drop in  $\mu_0 H_C$  from 8.2 to 3.9 mT and a corresponding decrease in  $M_{RS}/M_S$  (Table 1).  $H_{CR}$  also decreases with interactions, such that the ratio  $H_{CR}/H_C$  does not increase significantly between *S1* and *S3*. Whereas there is little change in  $H_C$  between *S1* and *S2*,  $M_{RS}/M_S$  is slightly lower for *S2*. From this we conclude that interactions are important even at quite large spacings, in contradiction to numerical findings that the contribution of interactions is negligible in magnetite for spac-

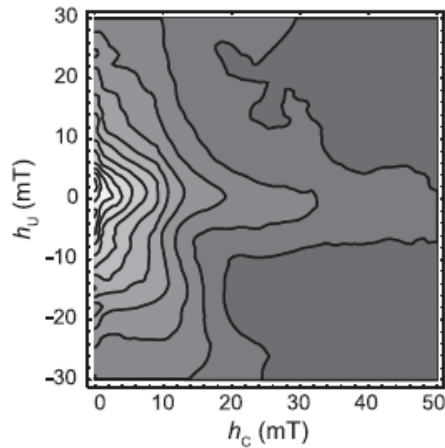


Figure 2. A FORC diagram for sample *A3*. The FORC diagram was measured parallel to grain elongation (see Table 1). The smoothing factor  $SF = 5$ , and the averaging time was 0.2 s. *A3* perpendicular was very similar in appearance to *A3* parallel and is not shown.

ings greater than approximately two times the grain size [Muxworthy *et al.*, 2003]. This difference may be due to a number of small differences between the model and the experiment: (1) lack of thermal fluctuations in the micromagnetic model, (2) a “quasi-static” numerical algorithm was used by Muxworthy *et al.* [2003] rather than a true dynamic model [e.g., Muxworthy and Williams, 2004], and (3) the model considered both smaller grains sizes and smaller arrays.

[17]  $H_{CR}/H_C$  is relatively unaffected by interactions while  $M_{RS}/M_S$  decreases resulting in a vertical downward shift on the Day plot with increasing interactions (Figure 1). This is in agreement with numerical models of cubic  $0.15 \mu\text{m}$  magnetic grains [Muxworthy *et al.*, 2003].

[18] In contrast to the two-dimensional interaction field in sample sequence *S1*, *S2* and *S3*, the one-dimensional “positive” interaction field in sample *A2* increases both  $H_C$  and  $M_{RS}/M_S$  compared to sample *A1*, which has identical noninteracting grains. When measured parallel to both the grain elongation and the interaction field  $H_C$  almost doubles in size. The interaction field also enhances the asymmetry of the hysteresis behavior of the  $3 \times 1 \times 1 \mu\text{m}$  grains;  $H_C$  parallel to the elongation is  $\sim 60\%$  bigger for *A2*, compared to only a  $\sim 20\%$  increase in the noninteracting *A1*. The ratio  $H_{CR}/$

$H_C$  also increases, causing both the perpendicular and parallel measurements of *A2* to plot on the upper right-hand-side of the respective *A1* measurements on the Day plot (Figure 1). The points measured at  $45^\circ$  are approximately intermediate to the measurements at  $0^\circ$  and  $90^\circ$  for sample *A2*.

#### 4. FORC Diagrams

[19] In recent years it has become common to construct FORC diagrams to characterize and un-

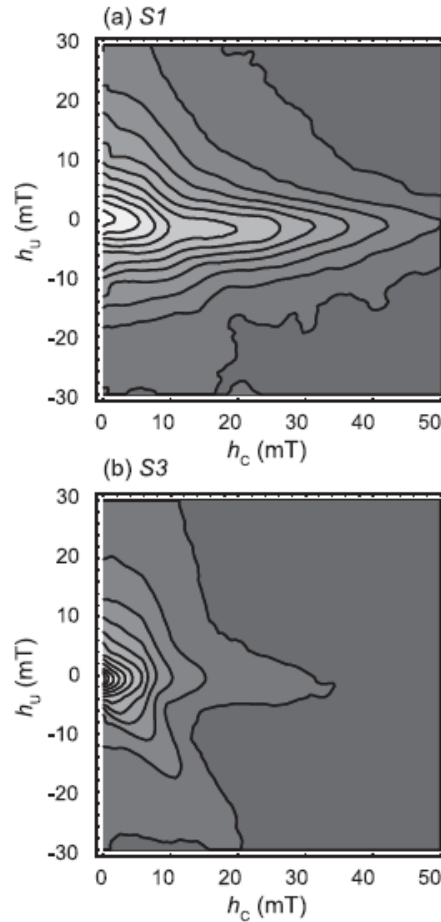


Figure 3. FORC diagrams for samples (a) *S1* and (b) *S3*. In both figures  $SF = 4$ , and the averaging time was 0.2 s.

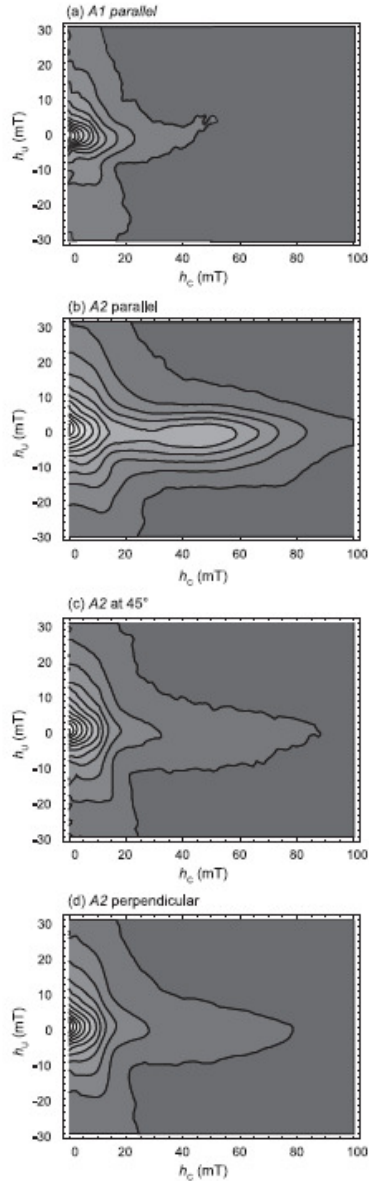


Figure 4. FORC diagrams for samples (a) *A1* parallel (to grain elongation), (b) *A2* parallel ( $0^\circ$ ), (c) *A2* at  $45^\circ$ , and (d) *A2* perpendicular ( $90^\circ$ ). In the figures, SF = 4, and the averaging time was 0.2 s. *A1* perpendicular was very similar in appearance to *A1* parallel and is not depicted.

derstand the magnetic signature of samples. A complete description of the measurement method, analysis and interpretations of FORC diagrams is given by *Roberts et al.* [2000] and *Muxworthy and Roberts* [2006]. As a first approximation, FORC distributions can be interpreted as the coercivity distribution along the horizontal axis ( $h_C$ ) and the interaction field distribution, along the vertical axis ( $h_U$ ). There is currently very little FORC data for well-characterized PSD magnetite samples. The EBL samples in this study provide a unique opportunity to assess FORC diagrams for small micron-sized magnetite grains and the contribution of interactions.

[20] The FORC diagram for *A3* with the field parallel to the elongation is shown in Figure 2. The FORC distribution lies very close to and is spread-out along the  $h_U$  axis, with a small tail extending along  $h_C$  axis. The FORC diagram for the field perpendicular to the elongation of *A3* is very similar in appearance to Figure 2 and is not depicted.

[21] By comparing the FORC diagrams for samples *S1* and *S3* (Figure 3), it is seen that the effect of two-dimensional interactions is to shift the FORC distribution closer to the  $h_U$  axis, and cause it to spread in the  $h_U$  direction. This general trend is in agreement with numerical models for SD assemblages [*Muxworthy et al.*, 2004].

[22] The contribution of linear/positive interactions is demonstrated in samples *A1* and *A2* (Figure 4). Figure 4a show the FORC diagram for *A1* measured parallel to grain elongation. The corresponding FORC diagram for *A2* is shown in Figure 4b, and the FORC diagram for *A2* measured at  $45^\circ$  and perpendicular to elongation in Figures 4c and 4d. The FORC diagram for *A1* with the field perpendicular to the elongation is very similar in appearance to Figure 4a and is not depicted. There is a much greater contrast between Figures 4b–4d. First, the later three FORC diagrams are extended further along the  $h_C$  axis compared to Figure 4a. Second, Figure 4b is extended noticeably further along the  $h_C$  axis than Figures 4c and 4d. Third, the FORC distribution in Figure 4b contains a second distinct peak/lobe at  $\sim 40$ – $50$  mT. That this peak is observed only in the parallel direction and not the perpendicular direction, suggests that this feature is due to interactions rather than undetected incomplete reduction to magnetite. Figure 4c is very similar in appearance to Figure 4d. Measurement of second-order reversals curves (SORCs) [*Newell,*

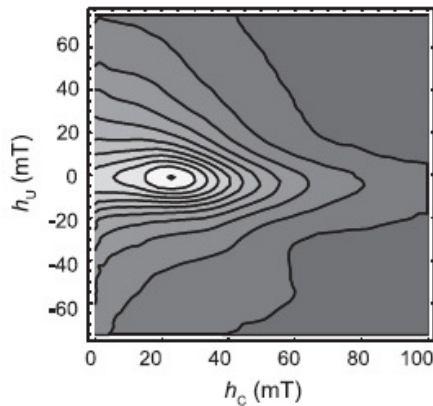


Figure 5. The  $W(1.7 \mu\text{m})$  is a powdered magnetite from Wright Industries and has a lognormal distribution with a mean grain size of  $1.7 \mu\text{m}$ . In this FORC diagram,  $SF = 3$ , and the averaging time was  $0.15 \text{ s}$ . Redrawn from *Muxworthy and Dunlop* [2002].

[2003] did not reveal any significant findings with respect to the switching mechanisms.

## 5. Discussion and Conclusions

[23] The role of planar/two-dimensional interactions is to make the hysteresis parameters  $H_C$  and  $M_{RS}/M_S$  decrease, and the FORC diagrams become more MD-like, however,  $H_{CR}$  does not correspondingly decrease, resulting in a vertical shift on the Day plot (Figure 1). This behavior was predicted for smaller  $0.15 \mu\text{m}$  interacting cubic grains from micromagnetic models [Muxworthy *et al.*, 2003].

[24] Measuring noninteracting asymmetric grains perpendicular to their elongation axis compared to parallel, produces more MD-like signals on both the Day and FORC diagrams (Figures 1 and 4). This is to be expected as both  $H_C$  and the  $M_{RS}/M_S$  ratio will decrease when measuring perpendicular to elongation. This effect is enhanced by interparticle interactions aligned with grain elongation (Figures 1 and 4).

[25] It is suggested that the second peak in Figure 4b is due to the uniform nature of the sample, and would not be observed in natural samples with wider distributions of interaction fields, grain sizes and coercive forces. Sample *A2* is effectively made up of chains ( $\sim 260$  in number)

of interacting grains, which due to interactions can be thought of individual magnetic systems. The switching distribution for the chains appears to be split in two. There are two mechanisms which could contribute to this effect. First, some chains switch at low-fields while others become trapped in meta-stable states until high fields are applied. The ability for a chain to reverse at low-fields may be due to an imperfection in the chain, e.g., a missing grain in the middle of the chain. In addition, it is probable that the small negative fields applied during the FORC measurement are insufficient to saturate the chains; instead “buckling” configurations in the chains will occur. On applying positive fields, these buckling configurations will switch at low fields giving rise to low coercivities. When larger negative fields are applied the magnetization of chains will reverse, giving rise to much higher switching fields.

[26] Compared to published FORC diagrams for powdered magnetite containing PSD grains, e.g., the  $W(1.7 \mu\text{m})$  sample shown in Figure 5, the general appearance of the EBL samples are more MD-like than the powdered sample with similar grain sizes, e.g., *S1* and *A3* (Figures 2 and 3). This is initially surprising as  $W(1.7 \mu\text{m})$  would be expected to be highly interacting being a powder, i.e., its FORC diagrams should spread in the  $h_U$  direction. In contrast, noninteracting samples *S1* and *A3*, appear more MD-like, even though in the case of *S1* it has a smaller mean grain size. It appears that in powdered samples such as  $W(1.7 \mu\text{m})$  the magnetic properties are dominated by the smaller particles in the grain-size distribution.

[27] Future studies will require a more complete set of electron beam lithography samples, which comprehensively covers the SD to PSD size range for symmetric and asymmetric grains, with various degrees of interaction fields.

## Acknowledgments

[28] The paper benefited from constructive reviews from Ramon Egli and David Heslop. A.R.M. is funded by the Royal Society.

## References

- Day, R., M. Fuller, and V. A. Schmidt (1977), Hysteresis properties of titanomagnetites: Grain size and compositional dependence, *Phys. Earth Planet. Inter.*, *13*, 260–267.
- Dunlop, D. J., M. F. Wescott-Lewis, and M. E. Bailey (1990), Preisach diagrams and anhysteresis: Do they measure interactions?, *Phys. Earth Planet. Inter.*, *65*, 62–77.

- Fernandez, A., M. R. Gibbons, M. A. Wall, and C. J. Cerjan (1998), Magnetic domain structure and magnetization reversal in submicron-scale Co dots, *J. Magn. Magn. Mater.*, *190*, 71–80.
- King, J. G. (1996), Magnetic properties of arrays of magnetite particles produced by the method of electron beam lithography (EBL), Ph.D. thesis, Univ. of Edinburgh, Edinburgh.
- King, J. G., and W. Williams (2000), Low-temperature magnetic properties of magnetite, *J. Geophys. Res.*, *105*, 16,427–16,436.
- King, J. G., W. Williams, C. D. W. Wilkinson, S. McVitie, and J. N. Chapman (1996), Magnetic properties of magnetite arrays produced by the method of electron beam lithography, *Geophys. Res. Lett.*, *23*, 2847–2850.
- Muxworthy, A. R., and D. J. Dunlop (2002), First-order reversal curve (FORC) diagrams for pseudo-single-domain magnetites at high temperature, *Earth Planet. Sci. Lett.*, *203*, 369–382.
- Muxworthy, A. R., and A. P. Roberts (2006), First-order reversal curve (FORC) diagrams, in *Encyclopedia of Geomagnetism and Paleomagnetism*, edited by D. Gubbins and E. Herrero-Bervera, Springer, New York, in press.
- Muxworthy, A. R., and W. Williams (2004), Distribution anisotropy: The influence of magnetic interactions on the anisotropy of magnetic remanence, in *Magnetic Fabric: Methods and Applications*, edited by F. Martín-Hernández et al., *Geol. Soc. Spec. Publ.*, *238*, 37–47.
- Muxworthy, A., W. Williams, and D. Virdee (2003), Effect of magnetostatic interactions on the hysteresis parameters of single-domain and pseudo-single-domain grains, *J. Geophys. Res.*, *108*(B11), 2517, doi:10.1029/2003JB002588.
- Muxworthy, A. R., D. Heslop, and W. Williams (2004), Influence of magnetostatic interactions on first-order-reversal-curve (FORC) diagrams: A micromagnetic approach, *Geophys. J. Int.*, *158*, 888–897.
- Newell, A. J. (2003), FORCs, SORCs and Stoner-Wohlfarth theory, *Eos Trans. AGU*, *84*(46), Fall Meet. Suppl., Abstract GP31B-0748.
- Pan, Q., T. G. Pokhil, and B. M. Moskowitz (2002), Domain structures in epitaxial (110) Fe<sub>3</sub>O<sub>4</sub> particles studied by magnetic force microscopy, *J. Appl. Phys.*, *91*, 5945–5950.
- Roberts, A. P., C. R. Pike, and K. L. Verosub (2000), First-order reversal curve diagrams: A new tool for characterizing the magnetic properties of natural samples, *J. Geophys. Res.*, *105*, 28,461–28,475.
- Yu, Y., L. Tauxe, and B. M. Moskowitz (2004), Temperature dependence of magnetic hysteresis, *Geochem. Geophys. Geosyst.*, *5*, Q06H11, doi:10.1029/2003GC000685.